

Optimal Investment in Preventative Capital to Control Episodic Air Pollution[†]

Ramjee Acharya^{*}

Arthur J. Caplan^{**}

April 6, 2017

Abstract: We address the issue of optimal investment in “preventative capital” to mitigate episodic, mobile-source air pollution events. We calibrate Berry et al.'s (2015) endogenous-risk model using a unique dataset related to "red air day" episodes occurring in Northern Utah over the past decade. Our analysis demonstrates that, under a wide range of circumstances, the optimal steady-state level of preventative capital stock – raised through the issuance of a municipal “clean air bond” that funds more aggressive mitigation efforts – can meet the standard for PM_{2.5} concentrations with positive social net benefits. We estimate benefit-cost ratios ranging between 0.9:1 and 2.2:1, depending upon trip-count elasticity with respect to preventative capital stock. These ratios are lower than the range estimated for the 1990 Clean Air Act Amendments in general.

Keywords: preventative capital; endogenous risk; PM_{2.5} concentrations; episodic air pollution

JEL Classifications: D62, Q53, Q58

[†] This study is funded in part by the Utah Agricultural Experiment Station (UTA0-1074 and UTA0-1334). The authors would like to thank participants at the 2016 Environmental and Resource Economics Workshop, University of Colorado, Eric Edwards, Sherzod Akhundjanov, Ryan Bosworth, and Man-Keun Kim for feedback on earlier versions of this paper. Any remaining errors are of course the authors' responsibility.

^{*} Department of Applied Economics, Utah State University, ramjee.acharya@aggiemail.usu.edu.

^{**} Corresponding author, Department of Applied Economics, Utah State University, arthur.caplan@usu.edu.

Optimal Investment to Control Episodic Air Pollution

Abstract

We address the issue of optimal investment in “preventative capital” to mitigate episodic, mobile-source air pollution events. We calibrate Berry et al.'s (2015) endogenous-risk model using a unique dataset related to "red air day" episodes occurring in Northern Utah over the past decade. Our analysis demonstrates that, under a wide range of circumstances, the optimal steady-state level of preventative capital stock – raised through the issuance of a municipal “clean air bond” that funds more aggressive mitigation efforts – can meet the standard for PM_{2.5} concentrations with positive social net benefits. We estimate benefit-cost ratios ranging between 0.9:1 and 2.2:1, depending upon trip-count elasticity with respect to preventative capital stock. These ratios are lower than the range estimated for the 1990 Clean Air Act Amendments in general.

1. Introduction

Although much is now known about the human health and environmental impacts associated with elevated air pollution concentrations during episodic outbreaks – both in general physiological terms and via copious dose-response studies conducted worldwide – relatively little research has been directed toward possible market-based economic policies that might effectively mitigate the costs associated with these outbreaks.¹ Both nation- and worldwide these costs are huge. An estimated 6.5 million pre-mature deaths occurred worldwide in 2012 due to elevated air pollution concentrations. Moreover, 90 percent of the world’s population is currently estimated to reside in locations where air pollution levels exceed the World Health Organization’s (WHO’s) ambient standards (WHO, 2017).² The annual mortality rate in the US alone due to elevated air pollution concentrations is estimated to be 200,000, of which over a quarter of the premature deaths are attributable to vehicle emissions (Caiazzo et al., 2013).

Recently, Moscardini and Caplan’s (2017) seasonal gas tax study and Cropper et al.’s (2014) piloted permit program have investigated specific market-based solutions to the prolific

¹ Pope et al. (2002) provide detailed estimates of the human health costs associated with elevated PM_{2.5} concentrations; estimates that corroborated by Utah Department of Environmental Quality (UDEQ) (2016e). See Liu et al. (2014) and Zanobetti and Schwartz (2009) (and references therein) for examples of dose-response studies. Morbidity and mortality estimates for US populations have since been compiled in the US Environmental Protection Agency’s (EPA’s) Environmental Benefits Mapping and Analysis Program (BenMAP) (2016a), which is used in this study to estimate health damages incurred by Northern Utah residents during episodic outbreaks.

² Roughly half of the 6.5 million deaths are in turn attributable to elevated PM_{2.5} concentrations, the specific pollutant considered in this study (Apte et al., 2015).

problem of mobile-source, episodic air pollution.^{3,4} The current paper extends this nascent strand of the literature by applying Berry et al.'s (2015) endogenous-risk, disease-outbreak framework to determine the optimal level of investment in “preventative capital” necessary to control mobile-source, episodic air pollution in Northern Utah, a region identified by the American Lung Association (ALA) as experiencing one of the nation’s worst short-term particulate pollution problems (ALA, 2017).⁵ The application of Berry et al.'s (2015) framework to the problem of mobile-source episodic air pollution is a natural and pertinent modeling extension given the measurable interplay between exogenous and endogenous risk factors associated with recurring “outbreaks” of elevated pollution events, which in turn induce similarly measurable impacts on human health.

In this paper we estimate the preventative capital stock necessary to optimally mitigate “red air day” episodes that occur during a typical winter inversion season; a capital stock raised

³ Even though the Utah Department of Environmental Quality (UDEQ) argues that the combination of (1) Tier-2 fleet standards and (2) local transportation plans to reduce vehicle miles travelled (VMT) and trips have the potential to reduce vehicle emissions by up to 50 percent by 2019 (UDEQ, 2016c), Moscardini and Caplan (2017) demonstrate why economic policies also directed toward reducing vehicle travel, such as their proposed seasonal gas tax for Cache County are likewise needed to mitigate red air day episodes. Moscardini and Caplan (2017) find that, on average, a one-percent decrease in county-level trip count results in a 0.75 percent reduction in $PM_{2.5}$ concentrations, all else equal. Further, a one-percent increase in gas price is correlated with a 0.31 percent reduction in vehicle trips. The authors estimate substantial seasonal social net benefits associated with this reduction. Their deadweight loss (DWL) estimate associated with the reduction ranges from \$2.5 - \$4 million, weighed against a median social benefit estimate of \$19.6 million. The authors also consider possible effects associated with the eventual adoption of Tier 3 technology for automobiles. They find that each five percent reduction in vehicle trips results in a \$0.56 (on average) reduction in the per-gallon tax (2012 dollars) necessary to eliminate a given season’s red air days on average. With Tier 2 technology in use, Cache County requires a 51% reduction in trip count to maintain the NAAQS for $PM_{2.5}$ concentrations.

Cropper et al.(2014) also investigate the use of a market-based policy to control episodic air pollution attributable to vehicle emissions, in their case ground-level ozone concentrations in Washington, DC. According to the authors’ estimates, their proposed permit scheme would remove one million vehicles from the road during high-ozone days, resulting in a corresponding reduction in NO_x emissions of 30 tons per day and generating an estimated \$111 million annually in government revenue, even in the face of non-compliance.

⁴ Studies assessing the efficacy of congestion pricing, or tolls, are nevertheless directly related to issue of controlling mobile-source pollution via a market-based instrument (c.f., Button and Verhoef, 1998; Phang and Toh, 2004; Anas and Lindsey, 2011).

⁵Here “episodic” refers specifically to clusters of “red air days” that occur intermittently throughout the winter months during temperature inversions. Red air days officially occur when particulate matter ($PM_{2.5}$) concentration levels exceed the National Ambient Air Quality Standards (NAAQS) of $35 \mu g/m^3$ during any given hour of the day.

through the issuance of, say, a municipal clean air bond. By “preventative capital stock” we mean the value of infrastructure associated with possible implementation of a future seasonal emission tax, a county-wide camera system, enhanced public transportation, more persuasive advertising encouraging people to become less reliant on their vehicles, subsidizing the purchase of zero-emission vehicles, etc., any or all of which would serve to control the future occurrence of red air day episodes.⁶ We calibrate a numerical version of Berry et al.’s (2015) model using a unique compilation of Northern Utah data for the period 2002 – 2012. This calibration exercise entails econometric estimation of the steady-state levels of background risk and red-air-day hazard rates associated with daily, winter, vehicle trip counts and relevant weather variables.

We estimate that Northern Utah’s optimal, steady-state preventative capital stock ranges from \$4 to \$14 million depending upon the assumed vehicle trip count elasticity with respect to preventative capital stock (with corresponding amortized annual values ranging from \$330,000 to \$1.13 million per year, respectively). The lowest trip-count elasticity assumed for this study (which is associated with an optimal preventative capital stock of \$4 million) results in a concomitant 13 percent decrease in the region’s vehicle trip count. The study’s largest elasticity (associated with an optimal preventative capital stock of \$14 million) corresponds to a 93 percent reduction in trip count. As expected, annual benefits associated with the concomitant decreases in PM_{2.5} concentrations track the reductions quite closely. Social net benefits (which are positive in eight of 10 scenarios considered in this study) increase monotonically with trip count elasticity, indicating that the more responsive is vehicle trip count to investment in preventative

⁶ Prevention in this case means restraining PM_{2.5} concentrations below the NAAQS during the inversion season. By comparison, prevention in Berry et al.’s (2015) model refers to the prevention of a possible disease outbreak. Our focus in this paper is on estimating the optimal stock of capital – a capital stock which can then be used to fund a variety of programs aimed at mitigating mobile-source pollution – not on how any particular program might subsequently be implemented. Program-by-program assessment is beyond the scope of this study.

capital, the larger the social net benefit. The corresponding benefit-cost ratios increase from 0.9:1 at the lowest trip count elasticity to 2.2:1 at the highest. These ratios are lower than EPA's (2011) estimated range for the 1990 Clean Air Act Amendments of between 3:1 and 90:1.

Elevated particulate matter (PM_{2.5}) concentrations have been a persistent, episodic pollution problem in Northern Utah's Cache County for the past several years (Figure 1 shows the county's location in the northern region of the state highlighted yellow. The red highlighted area is the state's fastest growing region, the Wasatch Front).⁷ As shown in Figure 2, which depicts the annual distributions of PM_{2.5} concentrations in the region during the 2002 – 2007 period (the period 2008 – 2012 depicts similar annual distributions), concentrations frequently spike above the National Ambient Air Quality Standards (NAAQS) of 35 µg/m³ averaged over any 24-hour period (horizontal red line) during the winter months (primarily December – February). The figure also reveals the variability in spikes from year to year. For instance, during the 2002, 2004, and 2005 inversion seasons spikes occurred more frequently, reaching markedly higher levels than those experienced in the 2003, 2006, and 2007 inversion seasons.

[INSERT FIGURES 1 AND 2 HERE]

Table 1 provides both the frequencies and relative frequencies of winter days in which PM_{2.5} concentrations exceeded the NAAQS for each year in our dataset. Commensurate with Figure 2, there is pronounced variability across years – during some years Cache County residents experienced a relatively large number of “red air days”, while during others the frequency was lower. Figure 3 shows the distribution of monthly average PM_{2.5} concentrations in Cache County for the years of our study, 2002 – 2012. Together, the two figures illustrate the episodic and seasonal nature of the region's red air day problem.

⁷ Logan is Northern Utah's largest city. In 2009, Logan's population consisted of 46,000 people residing in 16,000 households (U.S. Census Bureau, 2010). The population of Northern Utah is roughly 150,000.

[INSERT TABLE 1 AND FIGURE 3 HERE]

PM_{2.5} concentrations consist of dust and smoke particles. Short-term exposure to elevated PM_{2.5} concentrations is linked to increased hospital admissions and emergency department visits for respiratory effects, such as asthma attacks, as well as increased respiratory symptoms, such as coughing, wheezing and shortness of breath. In addition, short-term exposure is linked to reduced lung function in children and in people with asthma. Long-term exposure to elevated PM_{2.5} concentrations can cause premature death due to heart and cardiovascular disease associated with heart attacks and strokes. Some studies suggest that long-term exposure can cause cancer as well as harmful developmental and reproductive defects, such as infant mortality and low birth weight (EPA, 2016b; Dockery et. al, 1993; Pope et. al, 1995; Pope, 1989).⁸

The primary sources of PM_{2.5} concentrations in Northern Utah are vehicle exhaust, agricultural and industrial activities, and wood burning, the most pronounced of which is attributed to the former. As pointed out by Moscardini and Caplan (2017), during a typical inversion episode, anywhere from 60 to 85 percent of all PM_{2.5} is created by secondary particulate formation (UDEQ, 2016a). Secondary particulate formation occurs when precursor emissions of nitrogen oxides (NO_x), sulfur oxides (SO_x), and especially volatile organic compounds (VOCs) from vehicle emissions react and combine in the atmosphere to create concentrations of PM_{2.5} (UDEQ, 2016a). According to the Utah Department of Environmental

⁸ Utah residents concur that air quality is an insistent social concern. According to Envision Utah (2014 and 2013), Utah residents believe that mitigation of poor air quality should be the state's second highest priority, tied with funding of public education and only slightly behind management of water resources. Survey results indicate that, inter alia, over 60 percent of respondents believe air quality negatively impacts their lives, over 90 percent believe good air quality is integral in maintaining good health, and almost 80 percent believe air quality has worsened in the Greater Wasatch and Northern Utah regions over the past 20 years. Further, residents identify changes in how they transport themselves (i.e., changes in the extent to which they contribute mobile-source emissions), e.g., telecommuting, ridesharing, use of public transportation, reduced idling and unnecessary driving, as being the most beneficial approaches to improving air quality. Roughly 65 percent of respondents report that they would likely reduce the use of their vehicles if a tax increased the per-gallon price of gasoline by \$1.00; 32 percent indicating that they would be very likely to do so (Envision Utah, 2013 and 2014).

Quality (UDEQ), VOCs are highly reactive. As they break apart they combine with other gaseous chemicals to form nitrates. These nitrates then react with ammonia to form ammonium nitrate, the leading contributor to PM_{2.5} concentrations in the region. The UDEQ has therefore concluded that reducing vehicle VOC emissions offers the best near-term approach to reducing the region's PM_{2.5} concentrations during winter inversions (UDEQ, 2016a).

In geomorphic terms, inversions occur as the temperature at ground level falls beneath the temperature at higher elevations, trapping pollutants at the surface (UDEQ, 2016b). More specifically, as elevation rises temperature gradually decreases. Given conducive barometric-pressure, snowfall, snow depth, and wind-speed conditions, descending warm air creates an inversion layer. Within this layer, temperature increases with increasing elevation, constituting the reverse of normal air patterns. The inversion layer traps PM_{2.5} concentrations between geologic barriers which, in the case of Northern Utah, are the Wellsville and Bear River Mountain Ranges. A simplified depiction of a temperature inversion is provided in Figure 4.

[INSERT FIGURE 4 HERE]

In an effort to reduce vehicle emissions, county officials recently adopted a mandatory vehicle emissions testing program (VETP) – the efficacy of which has been hotly debated, primarily due to exemptions for diesel trucks (Anderson, 2013). To date, the VETP has been the sole mandatory initiative enacted by the state of Utah to control the region's red air day problem. Given Cache County's persistent non-attainment status for PM_{2.5} concentrations, the preponderant health impacts associated with equally persistent red air day episodes, and the relatively low expected efficacy of the county's VETP, the need to devise serious-minded policies to control these episodes is urgent. This paper demonstrates that, under a wide range of circumstances, the optimal, steady-state level of preventative capital stock necessary to fund

more aggressive mitigation efforts can meet the NAAQS with positive social net benefits. In the process of reaching this conclusion, we empirically estimate a series of models that not only measure the marginal impact of vehicle travel in the county, but also the impacts of a host of weather variables that are unique in explaining the red air day phenomenon.

The methodologies and empirical approaches developed in this paper are applicable to any region of the world where the control of mobile-source pollution is of public policy concern, more so where the pollutant is episodic in nature, as it is in several Latin American, Asian, and European cities (c.f., Gallego 2013a and 2013b; Ajanovic 2016), than where it occurs more regularly throughout the year, as in Beijing, China (see Cao et al., 2014 and Chen et al., 2013). Although the ultimate goal of our research is to empirically estimate the social net benefit of optimal investment in preventative capital, the various econometric components of the analysis, in particular regressions establishing linkages between air pollution concentrations, on the one hand, and vehicle usage and key weather variables on the other, are of stand-alone value.

As mentioned above, the problem of episodic air pollution is pervasive worldwide. WHO (2017) identifies mobile-source emissions as major contributors, particularly in several of the world's larger cities. By isolating the marginal impact of mobile-source emissions on episodic air pollution outbreaks in our study area, and by estimating the social net benefits associated with public investments to mitigate these impacts, our analysis therefore contributes to an on-going empirical assessment of what has become a widespread environmental problem driven by the necessity of transportation.

The next section presents a condensed version of the Berry et al. (2015) endogenous-risk model, tailored toward our “disease outbreak” of episodic pollution. Section 3 then discusses the data used in the empirical analyses underlying our subsequent calibration and numerical

simulations of the Berry et al. (2015) model. Section 4 presents our econometric results in support of calibrating the Berry et al. (2015) model, and Section 5 discusses our numerical results for optimal investment in, and the social net benefits associated with, preventative capital. Section 6 concludes.

2. Berry et al. (2017) Endogenous-Risk Model

As mentioned in Section 1, we adopt Berry et al.'s (2015) endogenous-risk model of disease outbreaks to estimate the optimal preventative investment rate and capital stock to control episodic red air days in Northern Utah. Following Berry et al. (2015), we let B represent (constant) annual county-level GDP and $z(t)$ represent preventative investment in time period t . Following an "outbreak" of a red air day episode, the county experiences subsequent annual environmental and health costs associated with that outbreak represented by $D(t)$, which can diminish over time.

Following repeated transformations, as discussed in Berry et al. (2015) and shown in greater detail in De Zeeuw and Zemel (2012) and Tsur and Zemel (1997), the region's maximization problem to determine optimal investment in preventative capital can be reduced to,⁹

$$\begin{aligned} \max_{z(t)} W &= \int_0^{\infty} [B - z(t) + \Psi(N(t), R(t))] e^{-rt - \gamma(t)} dt \\ \text{s. t. } \dot{N}(t) &= z(t) - \delta N(t), \dot{R}(t) = \sigma(R(t)), \dot{y}(t) = \Psi(N(t), R(t)), \\ N(0) &= N_0, R(0) = R_0, y(0) = 0, z(t) \geq 0, \end{aligned} \quad (1)$$

where, using B and $D(t)$ as defined above, $J = \int_0^{\infty} (B - D(t)) e^{-rt} dt$, i.e., J represents the present value of ex post net benefits given a red air day episode has occurred. Function

⁹ We refer the interested reader to these sources for further background on the specific derivations lying behind the ensuing equations. The framework itself was first developed by Reed (1987) and Reed and Heras (1992).

$\Psi(N(t), R(t))$ (with curvature conditions $\Psi_N < 0, \Psi_R > 0, \Psi_{NN} > 0, \Psi_{NR} > 0$, and $\Psi(N(t), 0) = 0$) represents the region's episodic hazard function, or instantaneous probability of a red air day occurring (described in more detail in Section 4.2), $y(t)$ denotes cumulative hazard function $\int_0^t \Psi(N(v), R(v)) dv$, r is the discount rate, $N(t)$ the level of preventative capital at time t (given initial level N_0), $R(t)$ the exogenous background risk of a red air day episode occurring at time t (given initial level R_0), and δ denotes the depreciation rate of capital. Net investment in preventative capital in period t is therefore defined as $\dot{N}(t) = z(t) - \delta N(t)$, and the evolution of background risk over time is denoted by function $\sigma(R(t))$.

As discussed in Berry et al. (2015) and Reed and Heras (1992), decision problem (1) is a deterministic, infinite-horizon optimal control problem solved through the application of Pontryagin's maximum principle (Kamien and Schwartz, 1991). The problem's objective function represents the discounted sum of expected net benefits from investment in preventative capital, where the discount factor $e^{-rt-y(t)}$ depends on both the economic, r , and risk-adjusted survival probability rates, $y(t)$. Each period's net benefit accounts for the expected return from transitioning to a red air day episode, $\Psi(N(t), R(t))J$. Hazard function $\Psi(N(t), R(t))$'s dependence on $N(t)$ denotes the mechanism through which the risk of a red air day episode occurring is endogenized.

A key innovation in our analysis will be to empirically estimate the steady-state level of background risk, R^{SS} , via probit regression analysis (following Greene (2018), Section 17.3), and Long and Freese (2014), Section 5.1) using our county-level dataset (described in more detail in Section 4). Hazard function $\Psi(N(t), R(t))$ will also be estimated based on this dataset following Greene (2018, Section 19.5.3) and Cleves et al. (2010, Section 3.1). To link the preventative

capital stock $N(t)$ with daily trip counts ($TC(t)$) within hazard function $\Psi(N(t), R(t))$, we assume a constant-elasticity formulation,

$$\ln(TC(t)) = A - c \ln(N(t)) \quad (2)$$

where $c \in (0.1, 1)$ represents the (absolute value) of trip-count elasticity with respect to preventative capital stock, and constant A is calibrated from (2) assuming median trip count for the region and $N(0) = \$1$ million.¹⁰

As Berry et al. (2015) show, the solution to maximization problem (1) can be written as,

$$z(N, R) = \delta N + \left[-\rho_2(N, R) - \frac{\Psi_{R(N,R)}}{\Psi_{N(N,R)}} \left(1 - \varepsilon_{\Psi} \frac{\gamma(N,R)}{N} \right) \right] \frac{\sigma(R)}{1 - \gamma_{N(N,R)}}, \quad (3)$$

where $\varepsilon_{\Psi} = |\Psi_{RN}(N, R)(N/\Psi_R(N, R))|$ is the (absolute value) of the elasticity of the hazard's response to R with respect to a change in N . This elasticity measures the relative endogeneity of risk associated with a red air day episode, i.e. the degree to which the impacts of background risk on the hazard rate can be managed via N . The larger the elasticity, the more effective is

preventative capital (Berry et al., 2015). Similarly, $\gamma(N, R) = \frac{r + \delta + \Psi(N, R)}{-\Psi_N(N, R)}$ and $-\rho_2(N, R) =$

$\frac{B - \delta N - rJ - [r + \Psi(N, R)]\gamma(N, R)}{\sigma(R)}$. Equation (3) therefore represents the investment feedback equation,

where in a steady state $\dot{R}(t) = \sigma(R(t)) = 0$ implies that $z(N, R) = \delta N$, i.e., investment in preventative capital just covers the portion of the capital stock that depreciates, and the bracketed term adjusts $z(N, R)$ on the steady-state trajectory.

As discussed in Berry et al. (2015), if the expression in the square bracket in equation (3) is positive then net preventive investment (i.e. $z - \delta N$) increases with background risk. The first

¹⁰ As we discuss in Section 6, we find some empirical evidence to support our presumed range for elasticity measure c . The range of trip-count elasticities adopted for this study represent a range of possible behavioral responses of drivers to different scales of investment in preventative capital. Since $N(0)$ is chosen arbitrarily for this analysis, we sensitize the analysis to alternative values, $N(0) \in [\$500,000, \$1 \text{ million}]$.

term in brackets, $-\rho_2(N, R)$, is the shadow value of increasing background risk, which is positive, i.e., the larger the background risk, the larger is the net investment required to prevent an episodic outbreak. The ratio $\frac{\Psi_R(N, R)}{\Psi_N(N, R)}$ represents the rate of substitution of N for R in managing the hazard rate, which is negative.

To determine the optimal steady-state preventative capital stock, we follow Berry et al. (2015) in utilizing the theoretical model's two steady-state equations,

$$\dot{N}(t) = z(t) - \delta N(t) = 0 \quad (4)$$

$$\sigma(R(t)) = R(t)\left(1 - \frac{R(t)}{R^{SS}}\right) = 0 \quad (5)$$

Combining equations (3) and (4) results in

$$\left[-\rho_2(N, R) + \frac{\Psi_R(N, R)}{-\Psi_N(N, R)} \left(1 - \varepsilon_\Psi \frac{\gamma(N, R)}{N}\right)\right] \frac{\sigma(R)}{1 - \gamma_N(N, R)} = 0. \quad (6)$$

Next, equations (5) and (6) are solved simultaneously to obtain optimal steady-state preventative capital stock N^{SS} . Lastly, as in Berry et al. (2015) we use the law-of-motion equation for $\sigma(t)$ (equation (5) not set equal to zero) to explore the dynamics of increasing background risk over time. Letting initial background risk be relatively close to zero, in particular $R(0) = 0.005$, and using $\sigma(t)$ to update $R(t)$ over time, the background risk (at the end of) period 1 is given by $R(1) = R(0) + \sigma(0)$, where $\sigma(0) = R(0)\left(1 - \frac{R(0)}{R^{SS}}\right)$, and similarly for $R(2)$, $R(3)$ and so on. The corresponding $z(t)$ values can then be calculated for given N^{SS} using equation (3).

3. Data

The data used in the empirical analyses presented in Section 4 are compiled from several different sources. Each variable in the dataset consists of a daily time step for the years 2002 –

2012.¹¹ Since the problem addressed in this study occurs seasonally each year (from December – February) we restrict the dataset to these months. PM_{2.5} concentrations are recorded hourly for Cache County by the Utah Division of Air Quality (UDAQ) at EPA station code 490050004 located in downtown Logan (UDEQ 2016c).

The weather variables – consisting of temperature gradient, wind speed, humidity, snow depth and snowfall level – were obtained from the Weather Underground and the Utah Climate Center (Weather Underground, 2016; Utah Climate Center, 2017). Lastly, vehicle trip count data was obtained from Utah Department of Transportation (UDOT, 2014). The Automatic Traffic Recorder (ATR) stations for the trip count data in Cache County are #303, #363, and #510. Figure 5 identifies the specific locations of the various stations in Cache County.

[INSERT FIGURE 5 HERE]

The summary statistics for and specific definitions of the variables used in our ensuing regression analyses are presented in Table 2. As indicated, the average daily PM_{2.5} concentration in Cache County during the winter months each year is 19.5 µg/m³ (recall that the NAAQS is 35 µg/m³). Average daily trip count (*TC*) is 40,538 (the natural log of this value is 10.61), whereas the average for the threshold indicator variable *Y* is 0.15 (meaning that roughly 15 percent of the sampled days are red air days).¹² The weather variables *WIND*, *TEMP*, *HUMIDITY*, *SNOWFALL*, and *SNOWDEPTH* measure the average daily wind speed, temperature gradient,

¹¹ PM_{2.5} concentrations, vehicle trip counts, and the weather variables used in this study are reported by their various sources on an hourly basis. For the analyses we have created daily averages from the hourly data.

¹² Specifically, 40,538 is the average daily trip count across our entire dataset based on the ATRs reporting the largest trip counts per day. We chose the largest reported daily trip count rather than the average across all ATRs because even the former measure is likely an underestimate of daily trips taken in the valley. This is due to the fact no one ATR is capable of recording all daily trips taken in the county. We were precluded from adding daily trips across all ATRs because of potential double-counting errors. It is important to bear in mind that even though our measure of daily trip counts is thus an underestimate in absolute terms, the measure exhibits no bias in relative terms across days. This fact is crucial for our analysis since it is the variability in trip count across days that we are interested in measuring in order to estimate trip count's marginal effect on the variability in daily PM_{2.5} concentrations.

humidity level, snowfall level, and snow depth occurring in Cache County during our study period. Weather variables are included as controls for relevant weather conditions determining $PM_{2.5}$ concentrations. *TEMP* is of particular importance. It is measured as the difference in temperatures between the region's high point (Mount Logan peak) and the valley's floor, i.e., a vertical temperature gradient. As discussed in Gillies et al. (2010) and Wang et al. (2015), a positive (or inverted) temperature gradient, where the air is colder near ground level and warmer at higher altitudes, is a key determinant of winter inversion conditions, in effect a necessary condition along with *SNOWDEPTH* and *SNOWFALL* for determining persistence of the region's wintertime red air day episodes.

[INSERT TABLE 2 HERE]

According to UDEQ (2018), a snow-covered valley floor reflects rather than absorbs heat from the sun, preventing normal mixing of warm and cold air and exacerbating the accumulation of $PM_{2.5}$ concentrations in the atmosphere. The deeper the snow depth the more heat is absorbed and the greater the positive effect on concentrations. Snowfall is coincident with lower air pressure, which in turn negatively affects $PM_{2.5}$ concentrations, all else equal. Calm winds reduce the mixing of warm and cold air and can also negatively affect concentrations, while higher levels of relative humidity are associated with higher concentration levels.

4. Empirical Analyses

In this section we present the empirical models used to estimate our data along with the corresponding results. We first estimate a Probit model using a subset of the variables contained in Table 1 in order to derive a mean estimate of the region's steady-state level of background risk, R^{SS} , described in Section 3. We then derive an estimate of the region's episodic hazard function $\Psi(N(t), R(t))$. As shown in Section 5, estimates of R^{SS} and $\Psi(N(t), R(t))$ are crucial

for our subsequent numerical simulations of the optimal steady-state preventative capital stock N^{SS} and corresponding investment in preventative capital, z^{SS} .¹³

4.1. Probit Analysis

Empirically, we can represent R^{SS} as the average probability of a red air day occurring in the region during the winter months. We proxy for background risk with the probability of a red air day occurring rather than merely the probable occurrence of a temperature inversion (as described in Section 3) because our data suggests that roughly 30 percent of red air days are not coincident with an inversion. Following Green (2018, Section 17.3) and Long and Freese (2014, Section 5.1), the probability of the occurrence of a red air day during the winter inversion season can be estimated according to,

$$Pr(Y = 1|\mathbf{X}) = \int_{-\infty}^{\mathbf{X}'\boldsymbol{\beta}} \phi(t)dt = \Phi(\mathbf{X}'\boldsymbol{\beta}), \quad (7)$$

where variable Y is as defined in Table 2, the functions $\phi(\cdot)$ and $\Phi(\mathbf{X}'\boldsymbol{\beta})$ represent the standard normal and cumulative standard normal distribution functions, respectively, and subscript t represents a given day. Matrix \mathbf{X} contains daily observations on the model's covariates (a subset of the variables defined in Table 2), and $\boldsymbol{\beta}$ is the corresponding vector of parameters to be estimated from the data. The corresponding likelihood function is specified,

$$Prob(Y_1 = y_1, Y_2 = y_2, \dots, Y_T = y_T|\mathbf{X}) = \prod_{y_t=0}[\mathbf{1} - \Phi(\mathbf{X}'\boldsymbol{\beta})] \prod_{y_t=1} \Phi(\mathbf{X}'\boldsymbol{\beta}), \quad (8)$$

¹³ We have chosen not to jointly estimate an underlying structural model linking determination of the region's steady-state background risk with its hazard function for two reasons. First, our underlying theoretical framework portrays background risk as an exogenous process. Thus, as in Berry et al. (2015), this risk factor is assumed to affect the hazard function exogenously, rather than as a joint determinant per se. Second, the probit and survival models estimated in this section are 'un-nested', in the sense that the categorical variable being determined in the former equation (whether or not a red air day has occurred) is not an endogenously determined explanatory variable in the latter equation (which itself determines the number of days until a red air day episode commences). As a result, any error correlation across these two equations potentially affects the efficiency of each equations' estimated coefficients not their accuracy.

which can be written more compactly as

$$L(\boldsymbol{\beta}|\mathbf{X}) = \prod_{t=1}^T [\Phi(\mathbf{X}'\boldsymbol{\beta})]^{y_t} [1 - \Phi(\mathbf{X}'\boldsymbol{\beta})]^{1-y_t}. \quad (9)$$

The log of (9) is given as

$$\ln L = \sum_{t=1}^T \{y_t \ln \Phi(\mathbf{X}'\boldsymbol{\beta}) + (1 - y_t) \ln[1 - \Phi(\mathbf{X}'\boldsymbol{\beta})]\}, \quad (10)$$

which estimates $\boldsymbol{\beta}$ using maximum likelihood.

The marginal effect of covariate $x_i \in \mathbf{X}$, $i = 1, \dots, I$, is then calculated as

$$\frac{\partial(\Pr(Y_t = 1|\mathbf{x}_i))}{\partial x_i} = \phi'(\mathbf{x}'_i\boldsymbol{\beta})\boldsymbol{\beta}_i, \quad (11)$$

where $\phi'(\mathbf{x}'_i\boldsymbol{\beta})$ is the marginal probability density function associated with $\Phi(\mathbf{X}'\boldsymbol{\beta})$ (Green, 2018, Section 17.3). R^{SS} is computed as the average of the predicted probability across observations. The estimated coefficients and associated marginal effects for our preferred specification of the model are presented in Table 3.¹⁴

[INSERT TABLE 3 HERE]

We begin by noting that the marginal effect of *TEMP* on dependent variable *Y* is of the expected sign (positive) and statistically significant at the one percent level. The higher the temperature gradient between Logan Peak and the valley floor, the higher the probability of a red air day occurring, all else equal, which conforms with Gillies et al. (2010) and Wang et al. (2015). The marginal effects for *LagPM_{2.5}*, *SNOWDEPTH*, and *HUMIDITY* are each also of the expected signs (positive) and statistically significant, while the coefficient for *SNOWFALL* is

¹⁴ We ran a host of other specifications for this model, including different sets of explanatory variables. We also tested for causal effects (endogeneity) associated with the *TEMP*, *HUMIDITY*, and *HUMWIND* weather variables, even though we know of no theory to suggest that *PM_{2.5}* concentrations partially determine these weather conditions. Results for these specifications were qualitatively similar to those reported in Table 3, particularly with respect to the estimation of R^{SS} , which is the key value being estimated in these regressions. Results for these models are available from the authors upon request. We used STATA version 14.1 for our regression analyses.

expectedly negative in sign and likewise statistically significant.¹⁵ The sign for *HUMWIND* is also expectedly negative but statistically insignificant.¹⁶

Most importantly for our purposes the model estimates that the average probability of a red air day occurring in the region during the winter inversion season as 16%. As mentioned above, the average probability measure is calculated as an average across daily predicted probabilities and serves as our estimate of steady-state background risk, R^{SS} . The pseudo R^2 and McFadden's R^2 values for this regression are both 60%, which is slightly above McFadden's Adjusted R^2 value. Akaike Information Criterion (AIC) and Bayesian Information Criterion (BIC) values are 225 and 256, respectively, and the Wald χ^2 test for at least one statistically significant coefficient in the model is significant at the 1% level. The model correctly predicts the positive outcomes of red air days 86% of the time, and negative outcomes (i.e., non-red air days) 94% of the time. The sample size for this analysis is 601.

4.2. Survival Analysis

Letting $G(\mathbf{X}(t))$ represent the probability of an episodic outbreak in period t , where $\mathbf{X}(t)$ is a vector of covariates from Table 2, the corresponding survival function is written as $S(t) = 1 - G(\mathbf{X}(t))$, and the hazard function $\Psi(\cdot)$ solves for the probability of an episodic outbreak given its non-occurrence prior to t .¹⁷ Following Berry et al. (2015), we define the hazard function in general as,

¹⁵ We also ran the model in Table 3 without *LagPM_{2.5}* as a regressor in order to assess the impact on the remaining regressors' coefficient estimates (as a test of *LagPM_{2.5}*'s potential endogeneity) and standard errors (as a test of potential serial autocorrelation). The results were qualitatively very similar. Further, the estimate for R^{SS} was 15.8 percent, also very similar to the 16 percent estimate from the model including *LagPM_{2.5}*. Lastly, we do not consider *TC* as an omitted variable from this model because it is uncorrelated with the remaining variables. As we discuss in Section 4.2, *TC* can instead be instrumented with either a weekday dummy or a series of day-of-the-week dummies.

¹⁶ Slight breezes stimulate the evaporation of water, leading to increases in humidity. Thus, we expected *HUMWIND* to exhibit a negative relationship with *PM_{2.5}*. *WIND* was included in an earlier specification and found to be statistically insignificant.

¹⁷ Because multiple red air day episodes typically occur in Northern Utah during the inversion season, we consider each episode as a special case and format the data accordingly (which is discussed in more detail below). Hence, the

$$\Psi(\mathbf{X}(t), R(t)) = R(t) \lim_{\Delta t \rightarrow 0} \left(\frac{\text{outbreak in } (t, t+\Delta t) | \text{no outbreak at } t}{\Delta t} \right) = \frac{R(t)g(\mathbf{X}(t))}{s(\mathbf{X}(t))}, \quad (12)$$

where $g(\cdot)$ is the probability density function (pdf) of $G(\cdot)$ and $R(t)$ again represents exogenous background risk. Following Barbier (2013), the hazard function is re-expressed as,

$$\Psi(\mathbf{X}(t), R(t)) = \frac{R(t)dG(\mathbf{X}(t))/dt}{s(\mathbf{X}(t))} = -\frac{R(t)\frac{dS(\mathbf{X}(t))}{dt}}{s(\mathbf{X}(t))} = -\frac{R(t)\dot{S}(\mathbf{X}(t))}{s(\mathbf{X}(t))} = -\frac{R(t)d \ln(S(\mathbf{X}(t)))}{s(\mathbf{X}(t))}. \quad (13)$$

Conditioning $\Psi(\mathbf{X}(t), R(t))$ on $N(t)$ post-estimation requires that a functional relationship be assumed between $TC(t)$ (which is a member of $\mathbf{X}(t)$) and $N(t)$. The conditioning occurs post-estimation because data on trip counts, rather than on preventative capital stock, is available for Cache County. Although a set of arbitrary relationships are therefore assumed to exist between $N(t)$ and $TC(t)$ for this study, we do find some empirical evidence to suggest that our chosen set includes those gleaned from relevant expense studies (APTA, 2014; Litman, 2011 and 2017; Pratt and Evans, 2004). We explain the functional relationship between $N(t)$ and $TC(t)$ in greater detail in Section 5.3.¹⁸

We test several standard parametric models for the ensuing survival analysis – exponential, Weibull, and Gompertz, as well as the semi-parametric Cox model. The Weibull hazard function (defined specifically as $\Psi(\mathbf{X}(t), R(t)) = R(t)pt^{p-1} \exp(\mathbf{X}(t)' \boldsymbol{\beta})$, where

wording “given no such outbreak has occurred prior to period t ” should, in a more technical sense, read “given no such outbreak has occurred prior to period t since the previous episode”. The episodes must be independently distributed in order to warrant such a statement, which in our case is evidenced by the statistically significant role that the weather variables (which are themselves exogenously determined) play in determining the start and finish of any given episode, as well as the episode’s duration and intensity. Hence, in our case survival is tracked between successive episodes during a given inversion season. As an example of what we mean by “successive episodes”, suppose the first episode in a given inversion season does not begin until day 20 and then lasts until day 23. Then the period during which no outbreak has occurred for the first episode (i.e., the first episode’s survival period) is days 1 to 19. If the second episode then begins on day 31, the associated survival period for the second episode is then days 24 to 30.

¹⁸ Notationally speaking, the post-estimation version of $\Psi(\mathbf{X}(t), R(t))$ is perhaps best written as $\Psi(\mathbf{X}(t), R(t); f(N(t)))$, where $f(N(t))$, which represents the functional relationship between $N(t)$ and $TC(t)$, is decreasing in $N(t)$.

parameter p represents the function's shape parameter and all other terms are as previously defined (Cleves et al., 2010, Section 3.1)) performed best in fitting our data.¹⁹

The occurrence of a series of daily $PM_{2.5}$ concentrations above the threshold $35 \mu\text{g}/\text{m}^3$ level in the region is considered an event in this study. For this analysis, a count-data variable must also be specified (Cleves et. al, 2010, Section 3.1); ours is defined as follows. After the first episodic outbreak, for example in December, we begin the count within a window during which $PM_{2.5}$ concentrations steadily increase, consecutively day-after-day, until the next episode occurs, i.e., our count-data variable is the number of steadily increasing days between red air day episodes. Similar counts are then taken between succeeding episodes.²⁰

The survival analysis results are presented in Table 4 for two versions of the Weibull model. In Weibull 1, potential endogeneity in TC is controlled with a weekday dummy variable for Monday – Friday as in Moscardini and Caplan (2017). In Weibull 2 the endogeneity is controlled with daily dummy variables for Monday through Friday. For both models we conducted standard Durbin-Wu-Hausman tests to establish the presence of potential endogeneity in the relationship between $PM_{2.5}$ and TC (Davidson and MacKinnon, 1993). The theoretical basis for TC 's endogeneity is premised on what is essentially routinized transportation behavior of the average household, i.e., trips for the most part are informally pre-scheduled for different days of the week, and fewer trips are taken valley-wide during weekends. Predicted trips subsequently used as regressors in each model are denoted as TC^* .

¹⁹ The Weibull hazard function exhibits the appealing property of increasing hazard over time for $p > 1$.

²⁰ It is important to note that spells between red air day episodes and the lengths of the episodes themselves each occur independently both within and between years. This is due to the fact that weather conditions, which are necessary for the emergence of the episodes, are exogenously determined. We also considered an alternative specification of the count-data variable, whereby the number of consecutive inversion days (i.e., days in which the Logan-peak temperature exceeds the valley floor temperature ($TEMP > 0$)) were counted between episodes. However, this approach unfortunately whittled our sample size down to a mere 21 observations. Results based on this count-variable specification are qualitatively similar to those presented in Table 4 and are available from the authors upon request.

[INSERT TABLE 4 HERE]

The coefficients for TC^* in both models are positive, indicating that on average an increase in the region's vehicle trip count increases the hazard of a red air day occurring. These effects are statistically insignificant, however, most likely due to the relatively small sample sizes of the regressions and relative coarseness of the trip count variable used in each model.²¹ The coefficients for $TEMP$, $SNOWDEPTH$, and $SNOWFALL$ are each of the expected signs and statistically significant. The positive effect of \ln_p in each model signifies that the hazard of a red air day occurring is monotonically increasing over the course of any given winter season in Northern Utah.

Comparing the AIC and BIC statistics across the two models, we base the ensuing numerical analysis of optimal investment in preventative capital on the Weibull 1 model, where the two statistics are lowest (Cleves et al., 2010, Section 3.1). In the numerical analysis, each of the covariates included in the Weibull 1 model are evaluated at their mean values, except for TC , which, as we now explain in Section 4.3 is expressed as a constant-elasticity function of N .

4.3. Relationship Between Vehicle Trip Count and Preventative Capital Stock

The assumed functional relationship between vehicle trip count (TC) and the value of preventative capital stock (N) in any period t is, as previously mentioned in Section 2, represented by equation (2). Despite the absence of studies looking specifically at the relationship between vehicle usage (measured either in terms of miles traveled or trips taken) and investment in preventative capital stock, we are able to glean some comparable estimates from studies that have at least touched on this issue. For example, APTA (2014) consider aggregate

²¹ TC is “coarse” in the sense that it serves as a proxy for vehicle-use decisions that are inherently made at the household level and yet is aggregated at the county level (recall that it is calculated as the total number of vehicle trips per day made in the region). In contrast, each weather variable is a non-aggregated, relatively precise scientific measurement of a meteorological occurrence.

savings in vehicle operating and fuel costs (associated with reduced vehicle usage) in response to expanded capital investment in public transport. In one scenario (the “Doubling Ridership Scenario”) where ridership increases by 3.53 percent per year, the associated elasticity (these authors’ own calculation) is 0.56. Under a “High Growth Scenario” where ridership increases by 4.67 percent per year the elasticity falls to 0.48. Similarly, Litman’s (2011) assessment of the Transport for London’s investment in a video camera network to manage congestion in Central London suggests an elasticity of roughly 0.2. Litman (2017) reports an average elasticity of transit use with respect to transit service frequency of 0.5, and elasticities with respect to service expansion ranging between 0.6 and 1. Taken together, these findings suggest that our chosen range for parameter $c \in (0.1,1)$ encompasses what empirical evidence is available.

We calibrate (2) such that the (A,c) combinations are based upon our data for $TC(t)$ and a rudimentary assumption about the current level of $N(t)$ in Cache County. Specifically, To generate values for parameter A for each assumed value of c we use the median number of daily vehicle trips per day in the region from our dataset, $TC(t = 0) = 40,216$. For $N(t = 0)$, we assume the region’s preventative capital stock presently stands at \$1 million, reflecting both the human capital (e.g., any city employee time directed toward promoting preventative activities city wide) and physical capital (infrastructure investments, including additional buses added to the county’s fleet that are used specifically during the inversion season to increase ridership, etc.).²² Using (2), we obtain the resulting (A,c) combinations presented in Table 5.

[INSERT TABLE 5 HERE]

²² We have also run separate simulations assuming $N(t = 0) = \$500,000$. Results based on this assumption are contained in Appendix Table A.1.

5. Estimates of the Optimal Preventative Capital Stock

We begin this section by completing the calibration of the theoretical model developed in Section 2. Toward this end, values are assigned to parameters δ , r , B , and J reflecting current conditions in Northern Utah, and the functional form for the background-risk motion equation, $\sigma(R(t))$, is chosen (Table 6 compiles the full set of calibrated values and functions used in our subsequent numerical analysis). We then solve the model numerically for the associated optimal steady-state levels of z and N . Lastly, we numerically derive the time path of z for the case of increasing background risk over time.²³

[INSERT TABLE 6 HERE]

As indicated in Table 6, we follow Berry et al. (2015) in assuming that exogenous background risk follows a logistic function. As mentioned in Section 4.2, Weibull Model 1 performs best in estimating hazard function $\Psi(N(t), R(t))$, which is parameterized with the corresponding coefficients provided in Table 4. The value for B is the Census Bureau's (2016) most recent estimate of Cache County's annual GDP; GDP being the best aggregate estimate of county-wide benefits at stake during red air day episodes. The value for J is then calculated as B net of average seasonal environmental damages (D) of \$63 million associated with an episodic outbreak in perpetuity. The estimate of \$63 million is calculated using the Environmental Benefits Mapping and Analysis Program (BenMAP) (EPA, 2016a). This benefit is based on the assumption that, on average, a reduction of 40 percent in $PM_{2.5}$ concentration is required to attain the NAAQS of no greater than $35 \mu\text{g}/\text{m}^3$ per day during the inversion season in Northern Utah (Moscardini and Caplan, 2017).²⁴ Thus, as in Berry et al. (2015), our measure of J captures the

²³ We use Matlab version R2016b (9.1.0.441655) 64-bit for our numerical analyses.

²⁴ For detailed information on the BenMAP facility visit <https://www.epa.gov/benmap>.

present discounted stream of social net benefits into perpetuity that remains after an outbreak has occurred (relative to no outbreak having occurred).

To determine the optimal steady-state preventative capital stock, we follow Berry et al. (2015) in utilizing the theoretical model's two steady-state equations,

$$\dot{N}(t) = z(t) - \delta N(t) = 0 \quad (14)$$

$$\sigma(R(t)) = R(t)\left(1 - \frac{R(t)}{R^{SS}}\right) = 0. \quad (15)$$

Combining equations (3) and (14) results in

$$\left[-\rho_2(N, R) + \frac{\Psi_R(N, R)}{-\Psi_N(N, R)} \left(1 - \varepsilon_\Psi \frac{\gamma(N, R)}{N}\right)\right] \frac{\sigma(R)}{1 - \gamma_N(N, R)} = 0. \quad (16)$$

Lastly, equations (15) and (16) are solved simultaneously to obtain N^{SS} .

Results for N^{SS} given the different (A, c) combinations presented in Table 5, along with corresponding optimal, steady-state vehicle trip counts (derived directly from equation (2), and henceforth denoted as TC^{SS}), are presented in Table 7.

[INSERT TABLE 7 HERE]

From Table 7 we see that the value of Cache County's optimal, steady-state preventative capital stock ranges from roughly \$4 to \$14 million depending upon the (A, c) combination. The corresponding amortized annual values ranges from \$330,000 to \$1.13 million per year.²⁵ In column 5, a social deadweight loss (DWL) is applied to the annual investments in preventative capital, reflecting both the region-wide social cost associated with raising revenue through the issuance of a county bond and the inefficiency calculated in Moscardini and Caplan (2017) corresponding to induced reductions in vehicle trips. To account for the DWL associated with the

²⁵ A 5 percent interest rate and 20-year loan term period are assumed for the amortization exercise.

issuance of a preventative-capital bond, we use the lower-bound DWL estimate of 20 percent (per dollar of revenue raised) reported in Campbell and Brown (2003). Campbell and Brown's (2003) estimate is in turn relatively conservative when compared with earlier DWL estimates reported in Findlay and Jones (1982), Freebairn (1995), Feldstein (1999), and Bates (2001). To account for the DWL associated with reduced vehicle trips we apply Moscardini and Caplan's (2017) estimate of \$267 per trip reduced to the number of reduced trips associated with an optimal capital stock, N^{SS} , reported in Table 7.

We consider our per-trip DWL estimate to be an upper-bound measure since the adjustment costs incurred by households, and indirectly by local businesses, in response to the trip-reducing incentives ultimately financed by the clean air bond (i.e., via the preventative capital investments) will likely diminish over time. This could occur, for instance, as households and businesses "learn by doing", or as preferences shift in favor of utilizing the low- and zero-emission technologies that will likely replace less-efficient technologies currently in use. Hence, the corresponding benefit-cost ratios we report below should be considered lower-bound.

It is interesting to note that although the county's optimal steady-state vehicle trip count decreases monotonically from approximately 35,000 trips per day to just under 3,000 as trip-count elasticity c rises from 0.1 to 1, the corresponding values of optimal steady-state preventative capital stock exhibit a non-monotonic relationship with the elasticity. The value rises from approximately \$4 million with an elasticity of 0.1 to just over \$14 million for an elasticity of 0.8, and then declines to just under \$14 million at an elasticity of 1. This divergent relationship between optimal trip count TC^{SS} and preventative capital stock N^{SS} is impelled, on the one hand, by the constant trip-count elasticity assumption (which drives the monotonic

decrease in TC^{SS}) and on the other by the diminishing (negative) effect of N on hazard function $\Psi(N(t), R(t))$ (which drives the non-monotonic pattern in N^{SS}).²⁶

The corresponding mean percentage changes in $PM_{2.5}$ concentration due to decreases in vehicle trip counts are calculated via Monte Carlo simulation using the ARMAX(1,0,0) and ARMAX (1,0,9) versions of Moscardini and Caplan's (2017) $PM_{2.5}$ regression equations.²⁷ The results in Appendix Table A.2 depict a positive relationship between reductions in vehicle trip counts and reductions in $PM_{2.5}$ concentrations for both the ARMAX(1,0,0) and ARMAX(1,0,9) models, denoted Models 1 and 2, respectively. The effects of weather variables $TEMP$, $SNOWFALL$, and $SNOWDEPTH$ on $PM_{2.5}$ concentrations are likewise as anticipated. The AIC and BIC statistics indicate that Model 1 fits the data best, hence we use the Monte Carlo results from this model to estimate the percentage changes in $PM_{2.5}$ concentrations associated with decreases in vehicle trip counts.

Recall the median trip count level for Cache County in our sample is roughly 40,000 trips per day. Hence, as shown in Table 7, at the lowest trip-count elasticity assumed for this study an optimal preventative capital stock of approximately \$4 million results in a concomitant 13 percent decrease in the county's vehicle trip count (from 40,216 to 34,924 trips). At the largest elasticity assumed in this study, an optimized \$14 million capital stock corresponds to a roughly 93 percent reduction in trip count.²⁸ Annual benefits associated with the concomitant decreases in $PM_{2.5}$ concentrations are calculated using BenMAP (EPA, 2016a). As anticipated, these

²⁶ The specific curvature conditions assumed for $\Psi(N(t), R(t))$ are provided in Section 2.

²⁷ The percentage change in $PM_{2.5}$ concentration is calculated as the mean of the sampling distribution of 10,000 sample means, where each sample consists of 90 observations (representing the length of the three-month winter inversion season) randomly drawn from respective normal distributions for each variable used in the ARMAX(1,0,0) equation, where the mean of the variable's distribution is the variable's sample mean.

²⁸ A trip count this low would have to be obtained with a large percent of zero-emission vehicles included in the region's fleet. This finding is not unlike the California Public Utility Commission's recent estimation that seven million electric vehicles will need to be on the road in order for the state to meet its 2030 greenhouse gas reduction goals (Walton, 2018).

benefits track the reductions in PM_{2.5} concentrations. Social net benefits are then calculated as the respective differences between annual benefits and the annual amortized values of the steady-state preventative capital stocks adjusted for deadweight loss. It is interesting to note that social net benefits increase monotonically with trip count elasticity, indicating that the more responsive is trip count to investment in preventative capital, the larger the social net benefit.²⁹

Corresponding benefit-cost ratios increase from 0.9:1 to 2.2:1.

Two aspects of our trip-count results bear mention. First, the data upon which key functions in the numerical model are based, in particular the hazard function, implicitly link the region's PM_{2.5} concentrations to the composition of the region's vehicle fleet during the period 2002 – 2012 in terms of vehicle models, ages, fuel-efficiencies, and emission-control technologies, etc. Thus, the optimal daily trip-count reductions derived here do not necessarily mean that trips themselves must decrease to those levels in today's terms. Rather, vehicle trips that produce emissions consistent with the fleet's composition during that time period (i.e., emissions-equivalent trips) must be reduced. Obviously, as more tier-three and zero-emission vehicles are included in the region's fleet over time, the magnitude of the reductions in vehicle trips necessary to meet the NAAQS threshold for PM_{2.5} concentrations (i.e., the associated emissions-equivalent trips) will naturally decrease (Moscardini and Caplan, 2017).

Second, it is interesting to note that Moscardini and Caplan (2017) estimate a required reduction to roughly 15,000 daily vehicle trips in order for Cache County to be in compliance with the NAAQS of 35 µg/m³ for an average inversion-season day. This threshold is closest to the optimal daily trip count level of 15,140 that we estimate for a trip-count elasticity of 0.4

²⁹ Social net benefit begins to diminish at $c = 7.5$.

(Table 7). Thus, Moscardini and Caplan's (2017) threshold estimate falls well within the range of optimal trip counts that we have estimated for this study.

Figure 6 presents a phase diagram corresponding to steady-state equations (15) (blue line) and (16) (grey line) for the case of $\rho_1 = 1$ (implying $z^{ss} \in (0, \infty)$), $c = 0.1$, and the parameter values and functional forms contained in Table 6. The steady-state equilibrium for this case occurs at the intersection of the two lines, corresponding to $N^{ss} = \$4.1$ million (from Table 7) and $R^{ss} = 16$ percent (from Table 3). The system's two eigenvalues (0.16 and -0.24), indicate a saddle-path equilibrium, depicted by the teal-colored arrowed line in the figure.

[INSERT FIGURE 6 HERE]

Lastly, as in Berry et al. (2015) we can appeal to the law-of-motion equation for $\sigma(t)$ from Table 6 to explore the dynamics of increasing background risk over time and its effects on the optimal investment in preventative capital. Letting initial background risk be relatively close to zero (at the end of period 0), in particular $R(0) = 0.005$, and using $\sigma(t)$ to update $R(t)$ over time, background risk (at the end of) period 1 is given by $R(1) = R(0) + \sigma(0)$, where $\sigma(0) = R(0)(1 - \frac{R(0)}{0.16})$, and similarly for $R(2)$, $R(3)$ and so on. The corresponding $z(t)$ values can then be calculated for given N^{ss} using (3) (we set $N^{ss} = \$4.1$ million for the analysis, which equals the N^{ss} value calculated from the simulation for $c = 0.1$), resulting in Figure 7 (y-axis is in billion \$). As indicated, investment for the initial period, $z(0)$, equals approximately \$3.8 million (evaluating (3) at $R(0)$). The investment level for the next period is $z(1) = \$0.5$ million, at which point the value of the preventative capital stock equals N^{ss} . Thus, for the remaining periods $z(t) = \delta N^{ss} = 0.05 \cdot \4.1 million = \$205,000 per period. Background risk continues increasing until reaching R^{ss} at the end of the eighth period.

[INSERT FIGURE 7 HERE]

6. Summary

This paper provides empirical estimates of the optimal investment in preventative capital to control episodic, wintertime, elevated PM_{2.5} concentrations in Northern Utah, a region recently identified by the American Lung Association (ALA) as experiencing one of the nation's worst short-term particulate pollution problems (ALA, 2017). The problem in this region is emblematic of similar problems faced throughout the world. Indeed, roughly 90 percent of the world's population is currently estimated to reside in locations where air pollution levels exceed the World Health Organization's (WHO's) ambient standards, with annual mortality rates attributed to these elevated pollution levels of over six million people (WHO, 2017).

For our study area we have estimated an average background probability of a red-air day occurring during the winter inversion season of 16%. We also estimate a positive relationship between the aggregate number of vehicle trips taken in the region and the hazard rate associated with exceeding the NAAQS PM_{2.5} concentration threshold of 35 µg/m³ on an average winter day. Theoretically expected correlations between exceeding the threshold, on the one hand, and a host of unique weather variables, on the other, are also established.

The value of Northern Utah's optimal, steady-state preventative capital stock is estimated to range from \$4 to \$14 million depending upon the assumed vehicle trip count elasticity with respect to investment in preventative capital (with corresponding amortized annual values ranging from \$330,000 to \$1.13 million per year, respectively). Further, we find that although the region's optimal vehicle trip count decreases monotonically from approximately 35,000 trips per day to just under 3,000 as trip-count elasticity rises, the corresponding optimal preventative capital stock exhibits a non-monotonic relationship with the elasticity. The value rises from just over \$4 million with an elasticity of 0.1 to just over \$14 million for an elasticity of 0.8.

At the lowest trip-count elasticity assumed for this study the optimal preventative capital stock of approximately \$4 million results in a concomitant 13 percent decrease in the region's vehicle trip count. At the study's largest elasticity an optimized \$14 million capital stock corresponds to a 93 percent reduction in trip count. As expected, annual benefits associated with the concomitant decreases in PM_{2.5} concentrations track the reductions quite closely. Social net benefits (which are positive for each scenario considered in this study) increase monotonically with trip count elasticity, indicating that the more responsive is vehicle trip count to investment in preventative capital, the larger the social net benefit. Corresponding benefit-cost ratios increase from 0.9:1 at the lowest trip count elasticity to 2.2:1 at the highest. These ratios are lower than EPA's (2011) estimated range for the 1990 Clean Air Act Amendments of between 3:1 and 90:1. As mentioned in Section 5, we consider our benefit-cost ratios to be lower-bound estimates as a result of our corresponding deadweight loss measures associated with reduced vehicle trips being upper-bound estimates.

Acharya and Caplan (2017) replicate this study's analysis for Utah's fast-growing, densely populated Wasatch Front region. The analysis for the Wasatch Front is complicated by the need to control for multiple county-level fixed effects in our estimation of background risk, hazard rate, and, ultimately, optimal steady-state investment in preventative capital. These types of replications in other regions of the world where episodic air pollution problems occur is one obvious avenue for future research, particularly where the type(s) of preventative capital and the scale of investment are relatively novel and large, respectively. It would be interesting to learn whether social net benefits are routinely positive under different circumstances than those considered in this study.

Of course to firm up the estimates of optimal investment, study locations need to measure the impact on vehicle usage of varying levels of preventative capital stock over time, preferably at the household level. It would be useful to measure household-level behavioral responses to these investments from the perspective of more accurately calibrating the endogenous-risk numerical model we have used to derive the social net benefit estimates, as well as from the perspective of simply learning the extent to which the investments induce both short- and longer-term changes in vehicle usage at the household level.

Finally, extending our analysis to account for the possible temporal impacts of climate change on local weather variables such as snowfall, snow depth, humidity, temperature, and wind (i.e., weather variables already serving as controls in our regression framework), is another logical direction that future research can take. For example, Lin et al. (2017), Chang et al. (2016), and Schroeder et al. (2017) estimate the impacts of climate variables on drought conditions in California, tropical cyclone activity, and predicted precipitation across the US, respectively. To the extent that the impacts of these climate drivers on local weather variables can similarly be estimated, our regression framework will ultimately permit us to project the effects of these impacts onto $PM_{2.5}$ concentrations, and thereby predict the attendant impacts of vehicle trip counts on the occurrence of red air days in the presence of climate change.

References

- Acharya, R. and A.J. Caplan (2017) Optimal investment in preventative capital to control episodic air pollution outbreaks: the case of the Wasatch Front, Utah's "red air day" problem. Unpublished manuscript, Department of Applied Economics, Utah State University.
- Ajanovic, A., R. Haas, and F. Wirl (2016) Reducing CO₂ emissions of cars in the EU: analyzing the underlying mechanisms of standards, registration taxes, and fuel Taxes. *Energy Efficiency* 9(4), 925-937.
- American Lung Association (ALA) (2017) State of the air. Retrieved from the Internet on June 12, 2017 at <http://www.lung.org/our-initiatives/healthy-air/sota/city-rankings/most-polluted-cities.html>.
- American Public Transportation Association (APTA) (2014) Economic impact of public transportation investment, 2014 update. Retrieved from the internet on March 12, 2017 at <https://www.apta.com/resources/reportsandpublications/Documents/Economic-Impact-Public-Transportation-Investment-APTA.pdf>.
- Anas, A. and R. Lindsey (2011) Reducing urban road transportation externalities: road pricing in theory and in practice. *Review of Environmental Economics and Policy* 5(1), 66-88.
- Apte, J.S., J.D. Marshall, A.J. Cohen, and M. Brauer (2015) Addressing global mortality from ambient PM_{2.5}. *Environmental Science and Technology* 49, 8057-8066.
- Barbier, E.B. (2013) Wealth accounting, ecological capital and ecosystem services. *Environment and Development Economics* 18(02), 133-161.
- Bates, W. (2001) How much government? The effects of high government spending on economic performance. New Zealand Business Roundtable, Wellington.
- Berry, K., Finnoff, D., Horan, R.D., and Shogren, J.F. (2015) Managing the endogenous risk of disease outbreaks with non-constant background risk. *Journal of Economic Dynamics & Control* 51,166-179.
- Button, K. and E. Verhoef (1998) *Road Pricing, Traffic Congestion and the Environment*. Northampton, MA: Edward Elgar Publishing Inc.
- Campbell, H.F. and R.P.C Brown (2003) *Benefit-Cost Analysis: Financial and Economic Appraisal Using Spreadsheets*. Cambridge University Press, Melbourne.
- Cao, J., X. Wang, and X. Zhong (2014) Did driving restrictions improve air quality in Beijing? *China Economic Quarterly* 13(3), 1091-1126.
- Carnovale, M., and M. Gibson (2013) The effects of driving restrictions on air quality and driver behavior. UCSD Working Paper Series, Department of Economics, University of California, San Diego, Available at <http://escholarship.org/uc/item/0v8813qm#page-1>

- Chang, C-W.J, S.-Y. Wang, and H.-H. Hsu (2016) Changes in tropical cyclone activity offset the ocean surface warming in northwest Pacific: 1981-2014. *Atmospheric Science Letters* 17(3), 251-257.
- Chen, Y., G.Z. Jin, N. Kumar, and G. Shi (2013) The promise of Beijing: evaluating the impact of the 2008 olympic games on air quality. *Journal of Environmental Economics and Management* 66, 424-443.
- Caiazzo, F., A. Ashok, I.A. Waitz, S.H.L Yim, S.R.H. Barrett (2013) Air pollution and early deaths in the United States. Part 1: Quantifying the impact of major sectors in 2005. *Atmospheric Environment* 79, 198-208.
- Cleves, M., Gutierrez, R.G., Gould, W., Marchenko, Y.V. (2010) *An Introduction to Survival Analysis Using Stata* (Third Edition). College Station, TX: Stata Press.
- Cropper, M. L., Jiang, Y., Alberini, A., and Baur, P. (2014) Getting cars off the road: the cost effectiveness of an episodic pollution control program. *Environmental and Resource Economics* 57, 117-143.
- Cummings, R.G. and M.B. Walker (2000) Measuring the effectiveness of voluntary emission reduction programmes. *Applied Economics*, 32(13), 1719-1726.
- Cutter, W.B. and M. Neidell (2009) Voluntary information programs and environmental regulation: evidence from “Spare the Air”. *Journal of Environmental Economics and Management*, 58(3), 253-265.
- Davidson, R. and J.G. MacKinnon (1993) *Estimation and Inference in Econometrics*. New York: Oxford University Press.
- De Zeeuw, A. and A. Zemel (2012) Regime shifts and uncertainty in pollution control. *Journal of Economic Dynamics and Control* 36(7), 939-950.
- Dockery, D.W., Pope, C.A., III, Xu, X., Spengler, J.D., Ware, J.H., Fay, M.E., Ferris, B.G., Speizer, F.A. (1993) An association between air pollution and mortality in six U.S. cities. *The New England Journal of Medicine*. 329(24), 1753-1759.
- Environmental Protection Agency (EPA), Office of Air and Radiation (2011) The benefits and costs of the clean air act from 1990 to 2020. Final Report – Rev.A. Retrieved from the internet on January 18, 2018 at https://www.epa.gov/sites/production/files/2015-07/documents/fullreport_rev_a.pdf.
- Environmental Protection Agency (EPA) (2016a) Environmental Benefits Mapping and Analysis Program (BenMAP). Retrieved from the internet on January 4, 2016 at <https://www.epa.gov/benmap>.
- Environmental Protection Agency (EPA) (2016b) Particle pollution and your health. Retrieved from the internet on June 14, 2016 at https://www.airnow.gov/index.cfm?action=particle_health.index
- Envision Utah (2014) 2014 values study results. Retrieved from the internet on November 16, 2015 at http://envisionutah.org/images/Values_study_release_1.pdf.

Envision Utah (2013) Utah air quality quantitative research results. Personal copy obtained from Envision Utah officials (with accompanying dataset) on January 4, 2014.

Feldstein, M. (1999) Tax avoidance and the deadweight loss of the income tax. *The review of Economics and Statistics* 81(4), 674-680.

Findlay, C. C. and R.L. Jones (1982) The marginal cost of Australian income taxation. *Economic Record* 58(162), 253.

Freebairn, J. (1995) Reconsidering the marginal welfare cost of taxation. *Economic Record* 71(213), 121–31.

Gallego, F., J.P. Montero, and C. Salas (2013a) The effect of transport policies on car use: a bundling model with applications. *Energy Economics* 40, S85-S97.

Gallego, F., J.P. Montero, and C. Salas (2013b) The effect of transport policies on car use: evidence from Latin American cities. *Journal of Public Economics* 107, 47-62.

Gillies, R.R., S-Y Wang, and M.R. Booth (2010) Atmospheric scale interaction on wintertime Intermountain West low-level inversions. *Weather Forecasting* 25, 1196-1210.

Greene, W. H. (2018) *Econometric Analysis* (Eighth Edition). New York: Prentice Hall.

Henry, G.T. and C.S. Gordon (2003) Driving less for better air: impacts of a public information campaign. *Journal of Policy Analysis and Management*, 22(1): 45-63.

Kamien, M.I. and N.L. Schwartz (1991) *Dynamic Optimization: The Calculus of Variations and Optimal Control in Economics and Management*. Advanced Textbooks in Economics, Amsterdam: Elsevier.

Lin, Y. L.E. Hipps, and S. Wang (2017) Empirical and modeling analysis of the circulation influences on California precipitation deficits. *Atmospheric Sciences Letters* 18, 19-28.

Litman, T. (2011) London congestion pricing: implications for other cities. Victoria Transport Policy Institute. Retrieved from the internet on March 22, 2017 at <http://www.vtpi.org/london.pdf>.

Litman, T. (2017) Evaluating public transit benefits and costs: best practices guidebook. Victoria Transport Policy Institute. Retrieved from the internet on March 24, 2017 at <http://www.vtpi.org/tranben.pdf>.

Liu, L., L-Y Yu, H-J Mu, L-Y Xing, Y-X Li, and G-W Pan (2014) Shape of concentration-response curves between long-term particulate matter exposure and morbidities of chronic bronchitis: a review of epidemiological evidence. *Journal of Thoracic Disease* 6 (Suppl 7), S720-S727.

Long, J.S. and J. Freese (2014) *Regression Models for Categorical Dependent Variables Using Stata* (Third Edition). College Station, TX: Stata Press.

Moscardini, L.A., and Caplan A.J. (2017) Controlling episodic air pollution with a seasonal gas tax: the case of Cache Valley, Utah. *Environmental and Resource Economics* 66(4), 689-715.

Osakwe, R. (2010) An analysis of the driving restriction implemented in San José, Costa Rica. Policy Brief, Environment for Development (EfD). Available at <http://www.efdinitiative.org/publications/analysis-driving-restriction-implemented-san-jose-costa-rica>.

Phang, S-Y and R.S. Toh (2004) Road congestion pricing in Singapore: 1975 to 2003. *Transportation Journal* 43 (2), 16-25.

Pope III, C. A., Burnett, R. T., Thun, M. J., Calle, E.E, Krewski, D., Ito, K., Thurston, G.D. (2002) Lung cancer, cardiopulmonary mortality, and long-term exposure to fine particulate air pollution. *The Journal of the American Medical Association*, 287(9), 1132-1141.

Pope, C.A., III, Thun, M.J., Namboodiri, M.M., Dockery, D.W., Evans, J.S., Speizer, F.E., Heath, J.C.W. (1995) Particulate air pollution as a predictor of mortality in a prospective study of U.S. adults. *American Journal of Respiratory and Critical Care Medicine*, 151(3pt1), 669-674.

Pope, C.A., III. (1989) Respiratory disease associated with community air pollution and a steel mill, Utah Valley. *American Journal of Public Health*, 79(5), 623-628.

Pratt, R.H. and J.E. Evans, IV (2004) Traveler response to transportation system changes. Chapter 10 – Bus Routing and Coverage. Transit Cooperative Research Program (TCRP) Report 95. Retrieved from the internet on March 14, 2017 at http://onlinepubs.trb.org/onlinepubs/tcrp/tcrp_rpt_95c10.pdf.

Reed, W.J. (1987) Optimal preventative maintenance, protection, and replacement of a revenue-earning asset. *Applied Mathematics and Computation* 24, 241-261.

Reed, W.J. and H.E. Heras (1992) The conservation and exploitation of vulnerable resources. *Bulletin of Mathematical Biology* 54(2/3), 185-207.

Schroeder, M., S.-Y. Wang, R.R. Gillies, and H.-H. Hsu (2017) Extracting the tropospheric short-wave influences on subseasonal prediction of precipitation in the United States using CFSv2. Forthcoming in *Climate Dynamics*.

Tsur, Y. and A. Zemel (1997) On event uncertainty and renewable resource management, in D. Parker and Y. Tsur (eds.), *Decentralization and Coordination of Water Resource Management*, Springer, US283-298.

Utah Climate Center (2016) Climate GIS|Station(s). Retrieved from the internet on March 20, 2017 at <https://climate.usurf.usu.edu/mapGUI/mapGUI.php>

Utah Division of Air Quality (UDAQ) (2015) Table 4: 2011 Triennial Inventory (tons/year). Retrieved from the internet on March 17, 2016 at http://www.airquality.utah.gov/info/annualreports/docs/2015/02Feb/Final_Annual_Report_2015.pdf.

Utah Department of Environment Quality (UDEQ) (2016a) Particulate Matter. Retrieved from internet on March 20, 2016 at <http://www.deq.utah.gov/Pollutants/P/pm/Inversion.htm>.

Utah Department of Environment Quality (UDEQ) (2016b) Information Sheet, p. 2. Retrieved from internet on March 10, 2016
<http://www.deq.utah.gov/Topics/FactSheets/docs/handouts/pm25sipfs.pdf>

Utah Department of Environment Quality (UDEQ) (2016c) Utah Air Monitoring Program. Retrieved from internet on March 10, 2016 at
<http://www.airmonitoring.utah.gov/network/Counties.htm>

Utah Department of Environment Quality (UDEQ) (2016d) Utah Division of Air Quality 2015 Annual Report. Retrieved from internet on September 23, 2016 at
http://www.deq.utah.gov/Divisions/daq/info/annualreports/docs/2015/02Feb/Final_Annual_Report_2015.pdf.

Utah Department of Environmental Quality (UDEQ) (2018) Inversions. Retrieved from the internet on January 11, 2018 at <https://deq.utah.gov/Pollutants/P/pm/Inversion.htm>.

Utah Department of Transportation (UDOT) (2014) Traffic statistics. Retrieved from the internet on August 26, 2014 at <http://www.udot.utah.gov/main/f?p=100:pg:::::1:T,V:507>.

United States Census (US Census) (2016) Quick Facts, Cache County Utah. Retrieved from the internet on March 17, 2015 at <http://www.census.gov/quickfacts/table/RHI805210/49005>.

Walton, R. (2018) SoCal electric vehicle pilots focus on heavy duty, fleet uses. UtilityDive.com. Retrieved from the internet on January 14, 2018 at <https://www.utilitydive.com/news/socal-edison-electric-vehicle-pilots-focus-on-heavy-duty-fleet-uses/514735/>.

Wang, S.-Y. S., Hipps, L. E., Chung, O.-Y., Gillies, R. R., Martin, R. (2015) Long-term winter inversion properties in a mountain valley of the western United States and implications on air quality. *Journal of Applied Meteorology and Climatology*, 54, 2339-2352.

Weather Underground (2016) About Our Data. Retrieved from the internet on March 6, 2016 at <http://www.wunderground.com/about/data.asp>.

Wolff, H. (2014) Keep your clunker in the suburb: low emission zones and adoption of green vehicles. *The Economic Journal*, 124, F481-F512.

World Health Organization (WHO) (2017) Media center. Retrieved from the internet on September 4, 2017 at <http://www.who.int/mediacentre/news/releases/2016/air-pollution-estimates/en/>.

Zanobetti, A. and J. Schwartz (2009) The effect of fine and coarse particulate air pollution on mortality: a national analysis. *Environmental Health Perspectives* 117, 898-903.

Zhang, W., C.-Y.C.L. Lawell, and V.I. Umanskaya (2016) The effects of license plate-based driving restrictions on air quality: theory and empirical evidence. Unpublished Working Paper. University of California at Davis. Retrieved from the internet on March 6, 2016
http://www.des.ucdavis.edu/faculty/Lin/driving_ban_paper.pdf.

Table 1. Frequency of winter days in which PM_{2.5} concentrations exceed 35 µg/m³.

Year	Number of Winter Days Above 35 µg/m ³	Percent of Winter Days Above 35 µg/m ^{3a}
2002 ^b	50	98
2003	11	13
2004	35	39
2005	28	31
2006	6	7
2007	11	13
2008	20	25
2009	23	28
2010	25	33
2011	11	13
2012	5	6
Median ^c	20 (13.73)	25 (25.81)

^aPercentages are based number of winter days for which data is not missing. The average number of non-missing winter days per year is 82.

^bPM_{2.5} concentrations were recorded on only 51 winter days in 2002.

^cStandard deviations are reported in parentheses.

Source: Moscardini and Caplan (2017).

Table 2. Variable definitions and summary statistics.^a

Variable	Description	Mean (SD)
<i>TC^b</i>	Log of daily trip count (# of vehicle trips).	10.61 (0.36)
<i>PM_{2.5}</i>	Daily PM _{2.5} concentration ($\mu\text{g}/\text{m}^3$).	19.56 (19.39)
<i>Y</i>	=1 if daily PM _{2.5} concentration is above 35 $\mu\text{g}/\text{m}^3$, 0 otherwise.	0.15 (0.36)
<i>TEMP</i>	Temperature gradient between Logan Peak and valley floor ($^{\circ}\text{F}$).	-7.30 (10.24)
<i>WIND</i>	Daily wind speed (miles/hour).	3.03 (2.67)
<i>HUMIDITY</i>	Daily humidity level (%).	82.67 (8.78)
<i>SNOWFALL</i>	Daily snowfall level (mm).	14.45 (37.54)
<i>HUMWIND</i>	HUMIDITY x WIND.	243.74 (203.89)
<i>SNOWDEPTH</i>	Daily snow depth (mm).	127.26 (115.87)

^a Standard deviations are in parentheses. The sample size is limited to 752 observations due to missing values for *SNOWDEPTH*.

^b *TC* is the log of maximum daily trip count as measured across the three ATR stations located in Cache County that consistently reported counts during our study period.

Table 3. Probit regression results.^a

Variable	Coefficients (SE)	Marginal Effects (SE)
<i>LagPM_{2.5}</i>	0.047*** (0.008)	0.004*** (0.001)
<i>TEMP</i>	0.057*** (0.012)	0.005*** (0.001)
<i>HUMIDITY</i>	0.035* (0.02)	0.003* (0.002)
<i>HUMWIND</i>	-0.001 (0.001)	-0.0001 (0.0001)
<i>SNOWFALL</i>	-0.01* (0.006)	-0.001* (0.001)
<i>SNOWDEPTH</i>	0.003*** (0.001)	0.0003*** (0.0001)
R^{SS}	16%	
Log pseudolikelihood	-105.36	
χ^2 (Wald)	136.57***	
Pseudo R ²	0.60	
Number of observations	601	
$\Omega_1 =$ Predictedredairday=1	0.86	
Observedredairday=1		
$\Omega_2 =$ Predictedredairday=0	0.94	
Observedredairday=0		
AIC	225	
BIC	256	
McFadden's R ²	0.60	
McFadden's Adj. R ²	0.58	

^a Dependent variable is Y from Table 2. Robust standard errors are in parentheses.
 ***, ** and * indicate significance at 1, 5 and 10% levels, respectively.

Table 4. Survival regression results.^a

Variable	Coefficients (S.E.)	
	Weibull 1	Weibull 2
<i>TC</i> *	0.476 (0.663)	0.151 (0.628)
<i>TEMP</i>	0.081*** (0.013)	0.080*** (0.013)
<i>SNOWDEPTH</i>	0.004*** (0.001)	0.004*** (0.001)
<i>SNOWFALL</i>	-0.01*** (0.004)	-0.01*** (0.004)
AIC	116.821	117.288
BIC	132.331	132.797
\ln_p	1.003 (0.077)	1.003 (0.077)
Number of observations	98	98

^a Robust standard errors are in parentheses, *TC** is predicted trips, and \ln_p is natural log of the Weibull shape parameter (see Section 4.2).
***, ** and * indicate statistical significance at 1, 5 and 10% levels, respectively.

Table 5. (A, c) combinations used in the numerical analysis.

c	0.1	0.2	0.3	0.4	0.5	0.6	0.7	0.8	0.9	1.0
A	9.91	9.22	8.53	7.84	7.15	6.46	5.77	5.08	4.39	3.69

Table 6. Parameter values and functional forms for the numerical analysis.

Parameter	Functional form/value	Source
R^{**}	16%	Probit analysis (Section 5.1)
$\sigma(t)$	$R(t)(1 - \frac{R(t)}{R^{ss}})$	Berry et al. (2015)
$\Psi(N(t), R(t))$	$R(t)pt^{p-1} \exp(\beta X(t)')$	Survival analysis (Section 5.2)
δ	0.05	Berry et al. (2015)
r	0.03	Berry et al. (2015)
B	\$ 2.39 billion	U. S. Census Bureau (2014)
D	\$63 million	BenMAP (EPA, 2016)
J	\$ 77.6 billion	$= \frac{B - D}{r}$
TC	$= \exp(A - c \log(N))$	Arbitrary

Table 7. Estimated N^{SS} values (million \$), associated TC^{SS} (daily county-level vehicle trips), and social net benefit (million \$).

c	A	N^{SS}	Annual N^{SS}	Annual N^{SS} + DWL	TC^{SS}	% Change in PM2.5	Annual Benefit	Social Net Benefit	Benefit/Cost Ratio
0.1	9.91	4.1	0.33	1.808	34,924	1.0	1.6	- 0.21	0.88
0.2	9.22	7.4	0.59	4.250	26,950	2.7	4.2	- 0.05	0.99
0.3	8.53	9.8	0.79	6.271	20,278	4.5	7	0.73	1.12
0.4	7.84	11.5	0.92	7.799	15,140	6.4	10	2.20	1.28
0.5	7.15	12.7	1.02	8.949	11,285	8.2	13	4.05	1.45
0.6	6.46	13.5	1.08	9.781	8,437	10.0	16	6.22	1.64
0.7	5.77	13.9	1.12	10.38	6,372	11.7	18	7.62	1.73
0.8	5.08	14.1	1.13	10.80	4,842	13.4	21	10.20	1.94
0.9	4.39	14.1	1.13	11.10	3,716	14.9	23	11.90	2.07
1	3.69	13.9	1.12	11.31	2,893	16.3	25	13.69	2.21

Figure 1. Cache County (highlighted yellow) and Wasatch Front (highlighted red).

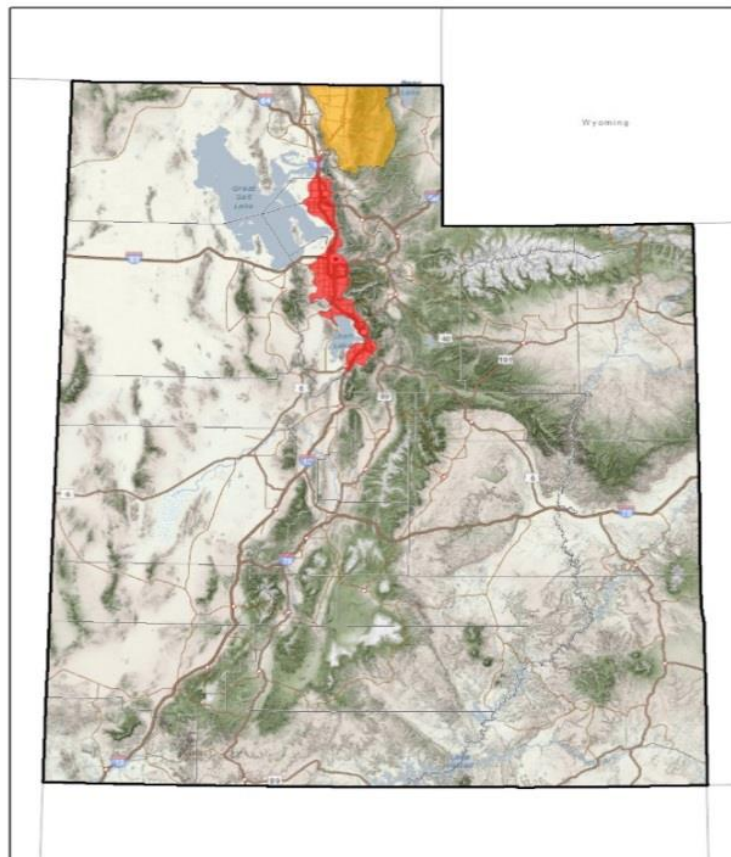
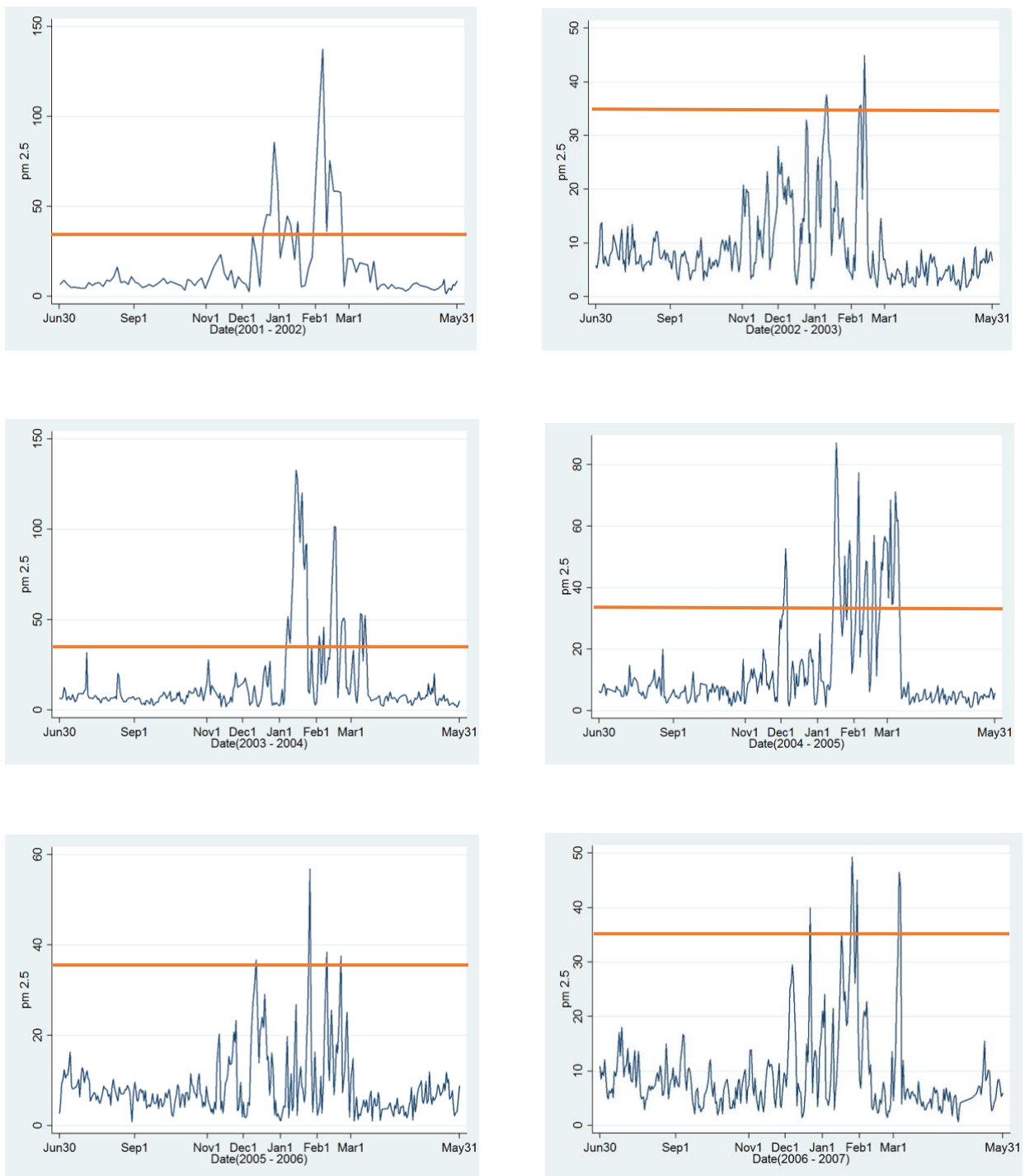
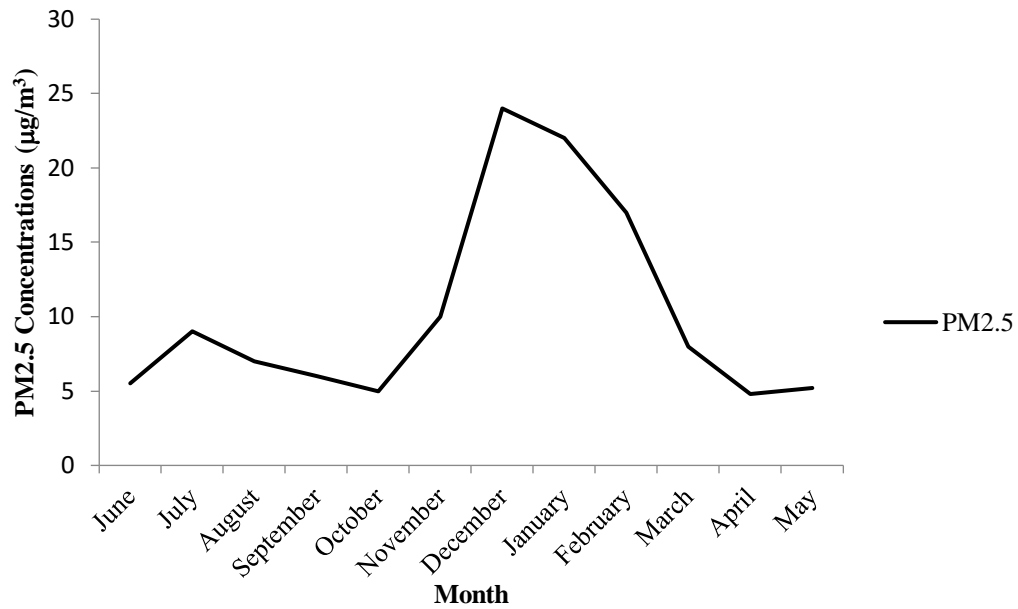


Figure 2. Annual PM_{2.5} concentrations in Cache Valley, Utah, 2002 – 2007.



Source: Moscardini and Caplan (2017).

Figure 3. Monthly average PM 2.5 concentrations for 2002 – 2012.



Source: Moscardini and Caplan (2017).

Figure 4. Winter inversion phenomenon in Northern Utah.

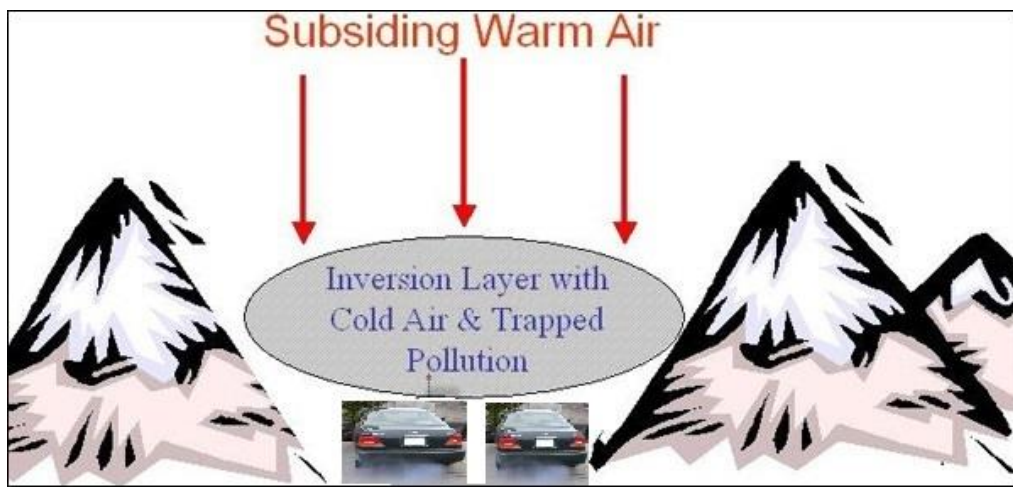
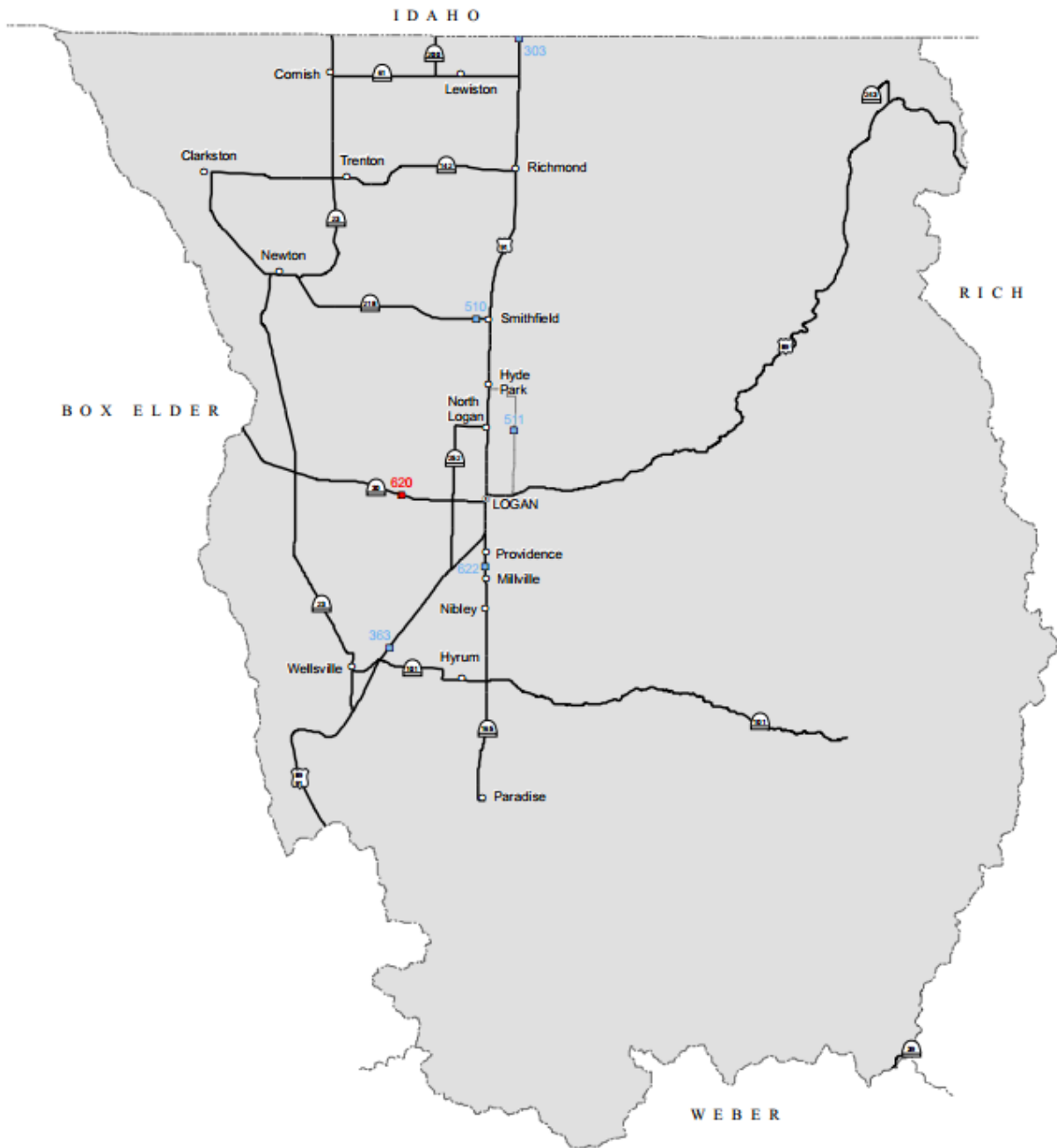


Figure 5. Automatic Traffic Recorder (ATR) station locations in Cache County, Utah.



Source: Moscardini and Caplan (2017).

Figure 6. Phase diagram for a steady-state equilibrium.

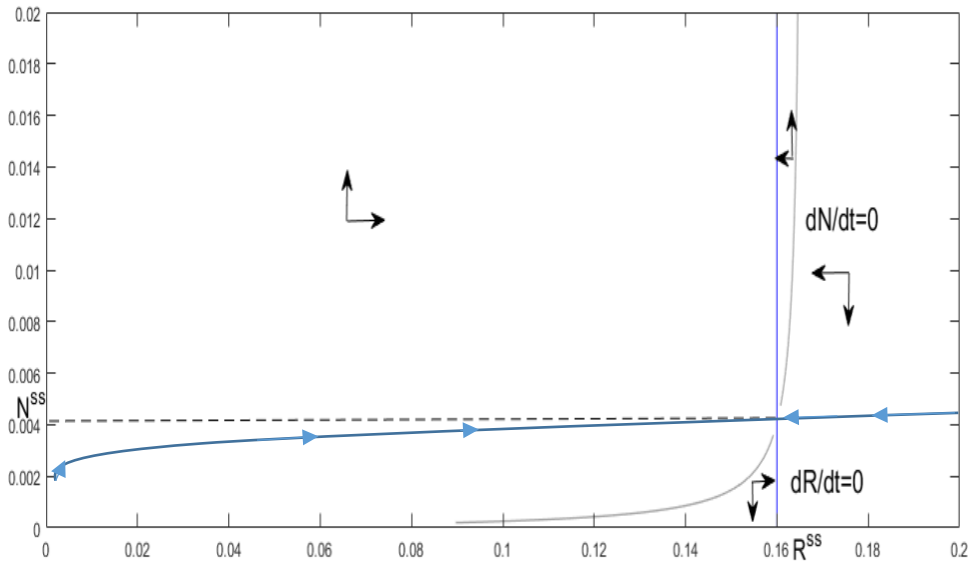


Figure 7. Time paths of $z(t)$ and $R(t)$ assuming increasing background risk over time.

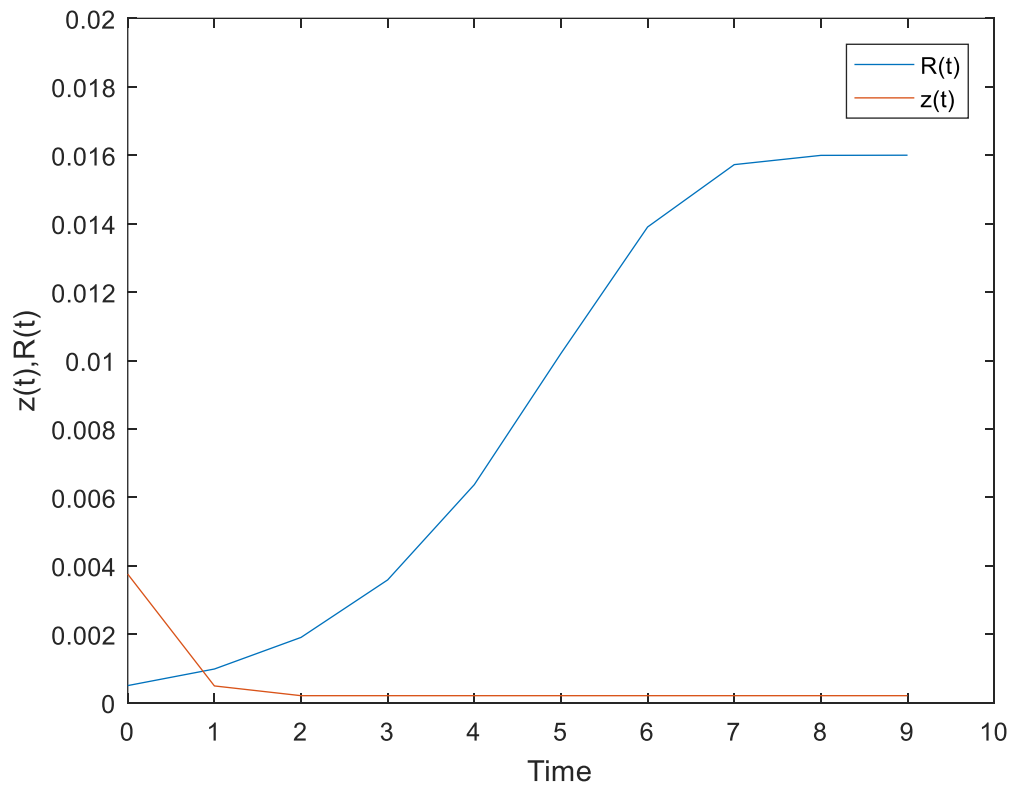


Table A.1. Simulation results for the case of $N(t = 0) = \$500,000$.*

c	0.1	0.2	0.3	0.4	0.5	0.6	0.7	0.8	0.9	1
A	9.84	9.08	8.32	7.56	6.80	6.04	5.28	4.52	3.76	3.00
N^{ss}	4	7	9	10	11	12	12	12	12	11
TC^{ss}	32,666	23,723	16,841	11,945	8,497	6,066	4,399	3,229	2,392	1,795

*As c increases the corresponding preventative capital stocks associated with $N_0 = \$500,000$ are everywhere lower than that associated with $N_0 = \$1,000,000$. The lower N^{ss} values associated with $N_0 = \$500,000$ case are driven by the lower corresponding A values for each c .

Table A.2. Regression results for Monte Carlo Simulation.^a

Variable	Coefficients (S.E.)	
	Model 1	Model 2
<i>TC</i>	0.17** (0.08)	0.23** (0.1)
<i>TEMP</i>	0.04*** (0.004)	0.05*** (0.004)
<i>SNOWDEPTH</i>	0.002*** (0.001)	0.002*** (0.001)
<i>SNOWFALL</i>	-0.004*** (0.001)	-0.004*** (0.001)
Log likelihood	-406.94	-401.59
χ^2 (Wald)	503.47***	12,981.88***
AIC	827.877	833.18
BIC	857.295	896.22
AR(1)	0.603*** (0.034)	0.98*** (0.028)
MA(1)		0.983 (1.36)
MA(2)		-0.87 (2.62)
MA(3)		-3.01 (5.89)
MA(4)		1.37 (9.0)
MA(5)		11.58 (--)
MA(6)		-4.69 (5.74)
MA(7)		0.27 (6.34)
MA(8)		-2.28 (7.95)
MA(9)		-3.30 (3.37)
Number of observations	494	494

^a Robust standard errors in parentheses.

***, ** and * indicate significance at 1, 5 and 10% levels, respectively.